Fuel 294 (2021) 120431

Contents lists available at ScienceDirect

Fuel

journal homepage: www.elsevier.com/locate/fuel

Full Length Article

Interactions in NO_X chemistry during fluidized bed co-combustion of residual biomass and sewage sludge

Burak Ulusoy [a,b,c], Bozidar Anicic [a,b,c], Weigang Lin [a,c], Bona Lu [c,d], Wei Wang [c,d], Kim Dam-Johansen [a], Hao Wu [a,*]

[a] Department of Chemical and Biochemical Engineering, Technical University of Denmark, Søltofts Plads 229, 2800 Kgs. Lyngby, Denmark
[b] Sino-Danish Centre for Education and Research, Beijing, China
[c] Sino-Danish College, University of Chinese Academy of Sciences, Beijing 100049, China
[d] Institute of Process Engineering, Chinese Academy of Sciences, Beijing, China

ARTICLE INFO

Keywords:
Biomass
Co-combustion
NO_X
Sewage sludge
Fluidized bed

ABSTRACT

This work investigates the interactions in NO_X chemistry during biomass co-combustion in a continuous lab-scale bubbling fluidized bed reactor. Co-combustion experiments were performed at air staged and unstaged conditions, and the gas composition in the flue gas and within the reactor was measured. The used biomass fuels were straw, sunflower husk, sewage sludge, and sunflower seed. Based on the NO concentration in the flue gas, straw-sunflower husk and straw-sunflower seed co-combustion were additive, while co-combustion of straw and sewage sludge revealed a synergy effect. The main cause was the presence of sewage sludge ash, which could catalyse the formation of NO from NH_3 and HNCO, and possibly HCN. The catalytic effect of the ash increased with lower ash preparation temperature and better mixing of the ash with straw. During straw-sewage sludge co-combustion, the NH_3 initially released from sewage sludge favoured the reduction of NO, while at later stages, when a significant amount of ash accumulated in the bed, the catalytic oxidation of NH_3 to NO was dominant. Compared to air unstaged conditions, the NO emission was reduced and the impact of ash on the nitrogen chemistry was less pronounced at air staged conditions.

1. Introduction

Biomass has received growing interest in heat and power production as it is a renewable and CO_2 neutral alternative to coal. However, the nitrogen content in different biomass may vary considerably, from 0.1 wt% for woody biomass to 11 wt% for aquatic biomass [1,2]. This could lead to increased emissions of nitrogen oxides, i.e. NO and NO_2 (NO_X), and N_2O, which have a detrimental impact on the environment, as NO_X are precursors for acid rain and photochemical smog, while N_2O is a greenhouse gas and ozone depleter [3,4]. In combination with the tightening regulations on NO_X emissions from biomass combustion, an improved understanding of the mechanisms of NO_X and N_2O formation and reduction during biomass combustion is of essential importance.

Fluidized bed combustion is a promising technology to utilize biomass for heat and power production, due to its high combustion efficiency and fuel flexibility [5]. In fluidized bed boilers, co-combustion of fuels is an important practice to improve performance and/or reduce fuel costs. While the interactions in combustion and ash chemistry during co-combustion have been extensively studied [6–10], the synergy effects in NO_X formation and reduction are much less understood.

Most of the literature, investigating the nitrogen chemistry in fluidized bed co-combustion, are focused on the combustion of coal and biomass. In these studies, a synergy effect was observed in the NO_X emissions, which generally decreased with an increase in the fuel volatile content [11–13], concentration of NH_i radicals [12,14], and char NO reduction reactivity [11,13,15]. In contrast, some studies have reported the absence of interaction between fuel particles of different origin, indicating that NO_X emissions from co-combustion are additive and therefore described by the propensity of the individual fuels for forming NO_X [16,17]. In most co-combustion studies, inferences related to NO_X chemistry are made based on the outlet NO concentration, which may hide interactions occurring locally within the combustor. This along with the lack of consensus on the existence of an interaction effect during co-combustion and the scarcity of fluidized bed biomass co-combustion studies provide the motivation for this work.

This study investigates NO_X emissions during co-combustion of different types of biomass in a lab-scale bubbling fluidized bed reactor.

* Corresponding author.
E-mail address: haw@kt.dtu.dk (H. Wu).

https://doi.org/10.1016/j.fuel.2021.120431
Received 13 July 2020; Received in revised form 27 December 2020; Accepted 6 February 2021
Available online 8 March 2021

Nomenclature

Abbreviations

d.b.	Dry basis
ID	Internal diameter
NO_X	NO and NO_2
Sew. slu.	Sewage sludge
Sunfl.	Sunflower
TDH	Transport Disengaging Height
VM	Volatile matter
w.b.	Wet basis

Symbols

C	Concentration [ppmv]
F	Fluegas from combustion of fuel [mol flue gas/kg fuel]
i	Index *i* used in the calculation of average NO emission
R	Fractional reduction [-]
u	Gas velocity [m/s]
w	Molar content [mol/kg]
x	Mass fraction [kg/kg]

Greek letters

λ	Excess air ratio
η	Selectivity (towards NO)

Subscripts

c	Combustion
g	Gas
in	Inlet
mf	Minimum fluidization
mix	Mixture of straw and secondary fuel
out	Outlet
S	Straw
sf	Secondary fuel
1	Primary

Continuous combustion experiments were performed at air staged and unstaged conditions. Effluent and local gas concentration data were measured, thereby providing a deeper understanding of the nitrogen conversion during biomass co-combustion. Straw was chosen as the base fuel for the co-combustion studies, since this, of the biomass studied, is commonly utilized industrially. Special emphasis was placed on the co-combustion using sewage sludge, due to its distinct interaction with other fuels.

2. Experimental

2.1. Materials

The properties of the investigated biomass, wheat straw, sunflower husk, sewage sludge, and sunflower seed, are shown in Table 1. The nitrogen and ash contents varied from 0.69 to 6.1 wt% and 3.2–50.2 wt %, respectively, thereby covering a wide range of nitrogen and ash contents in biomass. Wheat straw, sunflower husk, and sunflower seed pellets were grinded and sieved to a size range of 0.6–4 mm, while dried sewage sludge (0.5–2 mm) was used as received. These particle size ranges allowed for continuous sample admission, while minimizing fuel elutriation. Mixtures of fuels were prepared in a mechanical mixer for several hours prior to experiments. Silica sand was used as bed material (2600 kg/m^3, D_{50} 273 μm, Geldart B).

2.2. Sewage sludge ash and char preparation

To understand the behaviour of sewage sludge during co-combustion, sewage sludge ash and char were prepared.

Sewage sludge ash was prepared at three different temperatures (550, 850, 1000 °C) in a muffle furnace with continuous air supply (around 200 NmL/min). The total ashing time, i.e. from initiation until discontinuation of heating, was 5 h and 45 min, meaning that the heating rate was adjusted accordingly. The holding times at 550 °C, 850 °C, and 1000 °C were 5 h, 4 h, and 1 h, respectively, to ensure complete combustion. The absence of combustibles were confirmed by elemental (CHNS) analysis of the prepared ash.

Sewage sludge char was prepared in a horizontal oven at 850 °C with a N_2 flow of 2.5 NL/min. An alumina crucible containing approximately 10–20 g of sewage sludge was pushed into the preheated oven and kept there for 10 min [18,19]. After 10 min, the crucible was withdrawn to a water cooled section under N_2 atmosphere. The properties of the sewage sludge char are summarized in Table 2.

2.3. Setup

Continuous combustion experiments were performed in a stainless steel fluidized bed reactor illustrated in Fig. 1. The reactor consists of three sections, preheater (ID 100 mm), main reaction chamber (ID 61 mm), and upper freeboard (ID 100 mm). The fluidizing gas was heated in the preheating section and fed to the dense bed through a gas distributor. Biomass was continuously introduced to the reactor above the dense bed (300 mm above the gas distributor) using a screw feeder (K-Tron K-ML-KT20). To maintain stable fuel feeding, secondary gas was fed together with the fuel. The composition of the secondary gas varied and in the case air was used, the fuel feeding pipe was considered as the

Table 2
Properties of sewage sludge char. The char yield includes ash and fixed carbon, and was calculated based on the mass of solid sample prior and after charring.

	wt% d.b.							m^2/g
	C	H	N	S	O	Ash	Char yield	BET surface area
Sew. slu. char	14.51	0.46	1.48	0.16	0.51	82.9	54.6	53.1

Table 1
Fuel properties. VM: volatile matter, w.b.: wet basis, d.b.: dry basis.

Fuel	wt% w.b.	wt% d.b.								mg/kg d.b.							
	Moisture	VM	Ash	C	H	N	S	Cl	O	Al	Ca	Fe	K	Mg	Na	P	Si
Wheat straw	12.5	76.5	4.6	48.7	5.8	0.69	0.08	0.18	40.0	230	3600	180	8000	630	280	750	11,000
Sunfl. husk	9.1	75.8	3.2	51.7	5.7	0.80	0.14	0.04	38.4	55	3700	94	9600	2100	21	660	290
Sew. slu.	10.8	49.3	50.2	29	3.8	3.8	0.96	0.05	12.2	18,000	37,000	85,000	6300	4300	2400	34,000	75,000
Sunfl. seed	8.7	64.6	14	40.5	5.7	6.1	0.23	–	33.5	3095	3095	7328	18,416	6724	410	12,810	640

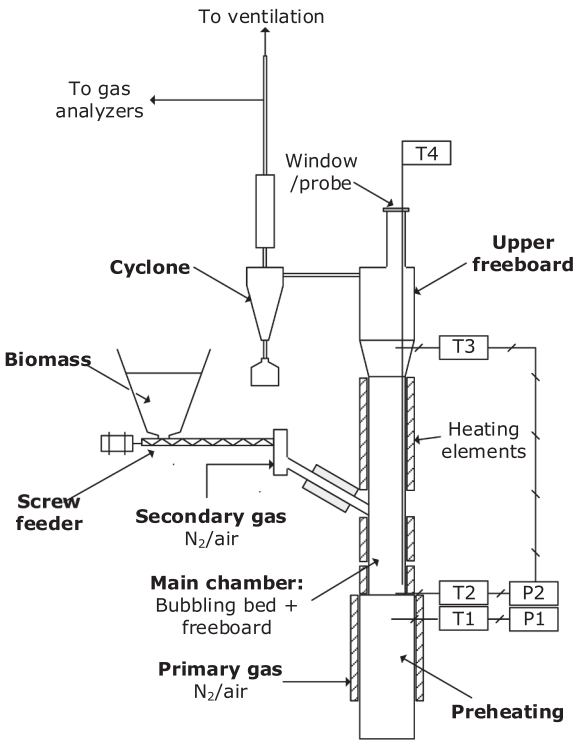

Fig. 1. Schematic of the bubbling fluidized bed reactor.

secondary air injection point. The flue gas was led through a cyclone to remove elutriated particles. One part of the exhaust gas was led to the gas analyzers (NGA2000, Fischer-Rosemount) to determine the flue gas concentrations of CO_2, CO, O_2, and NO, while the other part was sent to the ventilation. In selected cases, the total NO_x (NO and NO_2) was quantified (Eco Physics CLD 700 EL). As negligible amounts of NO_2 was measured (<1% of total NO_X), this was not further considered.

2.4. Experimental procedure

Approximately 0.5 kg of sand was used in each run, which corresponds to a static bed height of 10 cm. The bubbling bed height was around 12.5 cm and increased with the accumulation of ash, especially when combusting sewage sludge. The bed temperature was kept at 850 °C in all experiments by adjusting the external heating elements. Upon reaching the set point temperature, fuel feeding was initiated 30 cm above the air distributor. The fuel feeding rate was varied between 1.6 and 2.6 g/min, depending on the type of fuel to keep a constant excess air ratio (λ). The total amount of air supplied to the system was 11.5 NL/min, corresponding to $\lambda = 1.4$. At air unstaged conditions, all the air was introduced as primary gas ($\lambda_1/\lambda = 1$), while 15.5 NL/min of N_2 was fed through the fuel feeding pipe to facilitate the biomass feeding. In air staged experiments, half of the primary air was replaced with N_2 and the corresponding amount of air was supplied through the feeding pipe as secondary air ($\lambda_1/\lambda = 0.5$). Hence, the volumetric flow of gas in the system was kept constant to ensure comparable fluid dynamics, thereby leading to an operation velocity of about 4 times minimum fluidization velocity ($u_g/u_{mf} = 4$).

For most experiments, the axial temperature profile in the reactor was measured by a movable thermocouple (T4 in Fig. 1). The profiles were similar at all conditions, indicating a minor impact of temperature on the observations on the nitrogen chemistry. Examples of temperature profiles are shown in the supplemental material (Fig. S1).

Gas was sampled at different heights in the reactor using a water cooled probe inserted vertically from the top of the reactor. The local concentrations of different species, e.g·NH_3, CO, NO, NO_2, CH_4 etc., were measured by a Fourier Transform Infrared spectrometer (FTIR) (Multigas 2030 FTIR, MKS instruments). As no calibration for HCN was available, this was not measured. The repeatability of the local concentration measurements from straw combustion was reasonable as demonstrated in the supplemental material (Fig. S2).

3. Results and discussion

3.1. Air unstaged combustion

Fig. 2 illustrates the influence of biomass co-combustion on the averaged NO emission and fuel-N to NO conversion. The trend lines for the NO concentration and fuel-N to NO conversion were calculated using Eq. (1) and (2), respectively, assuming that the emission of NO was additive, i.e. determined by the propensity of the individual fuels for forming NO. The derivation of these equations is explained in the supplemental material (Additive NO equations).

$$C_{NO,mix} = \frac{(1 - x_{sf})C_{NO,S}F_S + x_{sf}C_{NO,sf}F_{sf}}{(1 - x_{sf})F_S + x_{sf}F_{sf}} \quad (1)$$

$$\eta_{mix} = \frac{C_{NO,mix}10^{-6}\left((1 - x_{sf})F_S + x_{sf}F_{sf}\right)}{x_{sf}w_{N,sf} + (1 - x_{sf})w_{N,S}} \quad (2)$$

Here, x_{sf} is the weight fraction of the secondary fuel, $C_{NO,S}$ and $C_{NO,sf}$ are the NO emissions (ppmv) during mono-combustion of the straw and secondary fuel respectively, $C_{NO,mix}$ is the calculated NO emission (ppmv) during co-combustion, F_S and F_{sf} are the moles of flue gas per mass of fuel (mol flue gas/kg fuel), $w_{N,S}$ and $w_{N,sf}$ are the molar nitrogen contents (mol N/kg fuel) in straw and secondary fuel, respectively, and η_{mix} is the calculated conversion of fuel-N to NO during co-combustion.

The results in Fig. 2a indicate that the NO emission from straw-sunflower husk and straw-sunflower seed co-combustion was additive as these follow the trend lines described in Eqs. (1) and (2). In contrast, the NO emission from straw-sewage sludge co-combustion exhibited a strong promoting effect (Fig. 2b). A similar synergy effect was observed in sunflower seed-sewage sludge co-combustion, shown in the supplemental material (Fig. S3). The promoting effect of sewage sludge was most likely caused by the catalytic effect of accumulated sewage sludge ash, in particular Fe and Ca, on NO formation from NH_3 and HCN oxidation [20–22]. Moreover, the CO emission, an indirect measure of reducing conditions and/or extent of mixing in the reactor, exhibited an inverse trend to the NO concentration during straw-sewage sludge co-combustion, which may contribute to the observed behaviour in NO [23]. In the following sections, the co-combustion with sewage sludge was further examined to elucidate the mechanism behind the interaction.

3.1.1. Influence of sewage sludge ash and char

To investigate the catalytic effect of sewage sludge ash, pellets of model compounds, urea and alanine, were introduced batchwise to the fluidized bed reactor before and after co-combustion experiments with sewage sludge. The bed before an experiment consisted of silica sand, while that after would additionally contain ash. Fig. 3 shows the conversion of model compound nitrogen to NO against the mass of sewage sludge ash theoretically added to the reactor during combustion. At a high heating rate, the decomposition of urea mainly yielded NH_3 and HNCO [24], while the major nitrogen product from alanine decomposition was NH_3 with a lesser amount of $CH_3CH_2NH_2$ [25]. The conversion to NO for both model compounds increased with the amount of ash added, indicating that the ash catalysed NO formation from NH_3 and HNCO. In addition, no significant differences were observed for the ash from straw-sewage sludge and sunflower seed-sewage sludge. This was most likely due to the higher ash content and possibly reactivity of sewage sludge (50.2 wt% d.b.) compared to that of straw (4.6 wt% d.b.) and sunflower seed (14 wt% d.b.). The conversion to NO levelled off

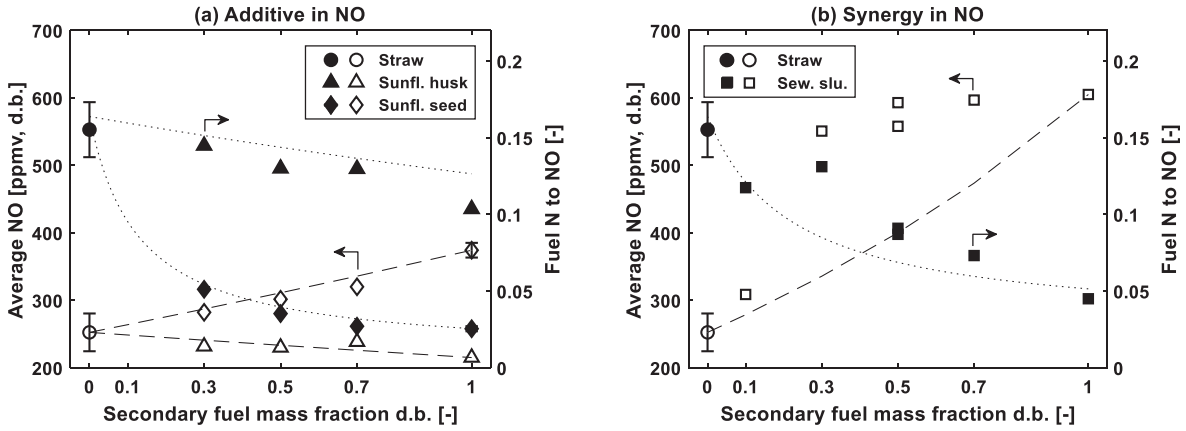

Fig. 2. Averaged NO emission (6% O_2) (open symbols) and fuel-N to NO conversion (closed symbols) during fluidized bed combustion of biomass. (a) illustrates the data additive in NO, while (b) shows the data exhibiting a synergy effect. Straw was the primary fuel. The trend lines were calculated assuming no interaction. The error bars on straw and sunflower seed were determined from several repetitions. Conditions: T_{bed} = 850 °C, λ = 1.4, λ_1/λ = 1.

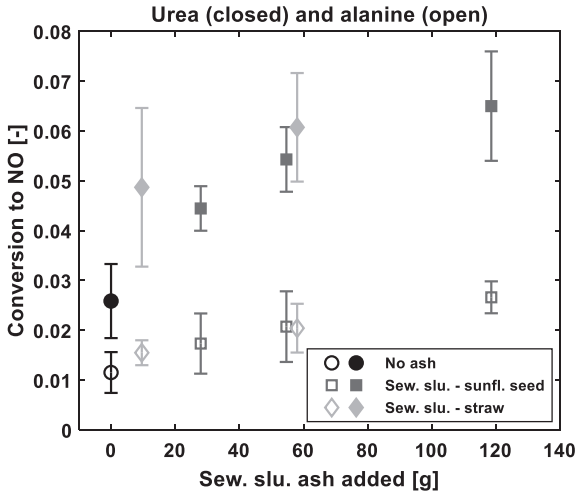

Fig. 3. Conversion of nitrogen to NO from combustion of urea (closed symbols) and alanine (open symbols) before and after continuous combustion experiments. Combustion experiments were continued for around 1.5 h. The error bars were determined from several repetitions. No ash refers to a fluidized sand bed. Conditions: T_{bed} = 850 °C.

with the amount of ash added to the reactor.

Fig. 4a illustrates the NO emission from combustion of straw with sewage sludge ash prepared at different temperatures. The ash particles were either added batchwise from the top of the reactor or premixed with the straw. The results show that the presence of sewage sludge ash increased the NO emission. The influence of ash was highest when the ash was premixed with the fuel and prepared at lower temperatures. To explain the influence of ash preparation temperature on the chemical and physical properties of ash, the BET surface area and XRD spectra were determined.

The ash specific surface areas at 550 °C, 850 °C, and 1000 °C were 17.8 m^2/g, 2.9 m^2/g, and 1.5 m^2/g, respectively, thereby decreasing with the severity of heat treatment. Fig. 4b demonstrates the NO emission during straw combustion with the batch addition of sewage sludge ash against the total ash surface area available in the reactor. The latter was calculated by multiplying the specific ash surface area with the ash mass at a given time. The results indicate that NO emission increases with the increase in available sewage sludge ash surface area, especially prominent for the high temperature (850 °C and 1000 °C) ash. Based on the results in Fig. 4a, the ash preparation temperature may not be the sole reason for the differences in reactivity and surface area of the ash. Since the 550 °C ash is exposed to 850 °C when entering the reactor, this would be expected to react similar to the 850 °C. However, based on the results in Fig. 4, this is not the case. This may be due to differences in the degree of ash sintering in the muffle furnace and fluid bed reactor. However, based on the present results no inferences can be made on the influence of sintering, and this may instead be the subject of future work. Another contributing factor to the different reactivities could be the differences in ash composition.

XRD results of the ash are shown in Fig. 4c, showing that the crystal structure of the ash prepared at 550 °C was different from the higher temperature ash. The low temperature ash contained $K_6Fe_2O_5$, while at higher temperatures, K was mainly bound to silicate compounds and Fe existed as Fe_2O_3. While little information is available on the catalytic effect of K-Fe-O species on NO formation from volatile-N, the form of ash/solids have been shown to have a strong influence on its catalytic influence [26,27]. Hence, further fundamental studies may be required to elucidate the influence of ash composition on NO_X reactions.

Besides ash preparation temperature, the ash introduction method was also of importance, as premixed ash increased the NO emissions to a larger extent compared to batch addition. Premixing would lead to a closer contact between the fuel and ash, thereby facilitating the catalytic conversion of fuel-N to NO. Premixing additionally reduced the effluent CO concentration (0.33%) relative to batch addition (0.64%) and raw straw combustion (0.65%), indicating less reducing conditions in the reactor during premixed combustion, which may contribute to the increased NO emission. The decrease in CO may be attributed to the catalytic effect of sewage sludge ash on CO oxidation [28] or to the capture of KCl from straw by sewage sludge ash [29], as KCl could inhibit CO oxidation [30].

In Fig. 4a, the NO emission was constant after the introduction of approximately 10–20 g of ash, suggesting a saturation effect. The mechanism of this effect is demonstrated in Fig. 4d showing that, as the bed is enriched by ash, the volatile matter is predominantly consumed nearby ash particles, thereby minimizing the influence of ash particles further away from the fuel particle. Moreover, transient changes in the NO emission during straw combustion with batch ash addition are demonstrated in the supplemental material (Fig. S4). These indicate that some deactivation of the 550 °C ash could be prominent, while negligible changes were observed for the higher temperature ash.

Fig. 5a and b display the NO emission and fuel-N to NO conversion, respectively, against the theoretical amount of sewage sludge ash added to the reactor during combustion of straw with sewage sludge and its derivatives, i.e., ash and char. The fraction of char in the premixed fuel (29 wt% d.b. of char) was calculated to ensure a constant sewage sludge ash feeding rate during experiment. The NO emission and fuel-N to NO conversion from the combustion of straw with sewage sludge ash and

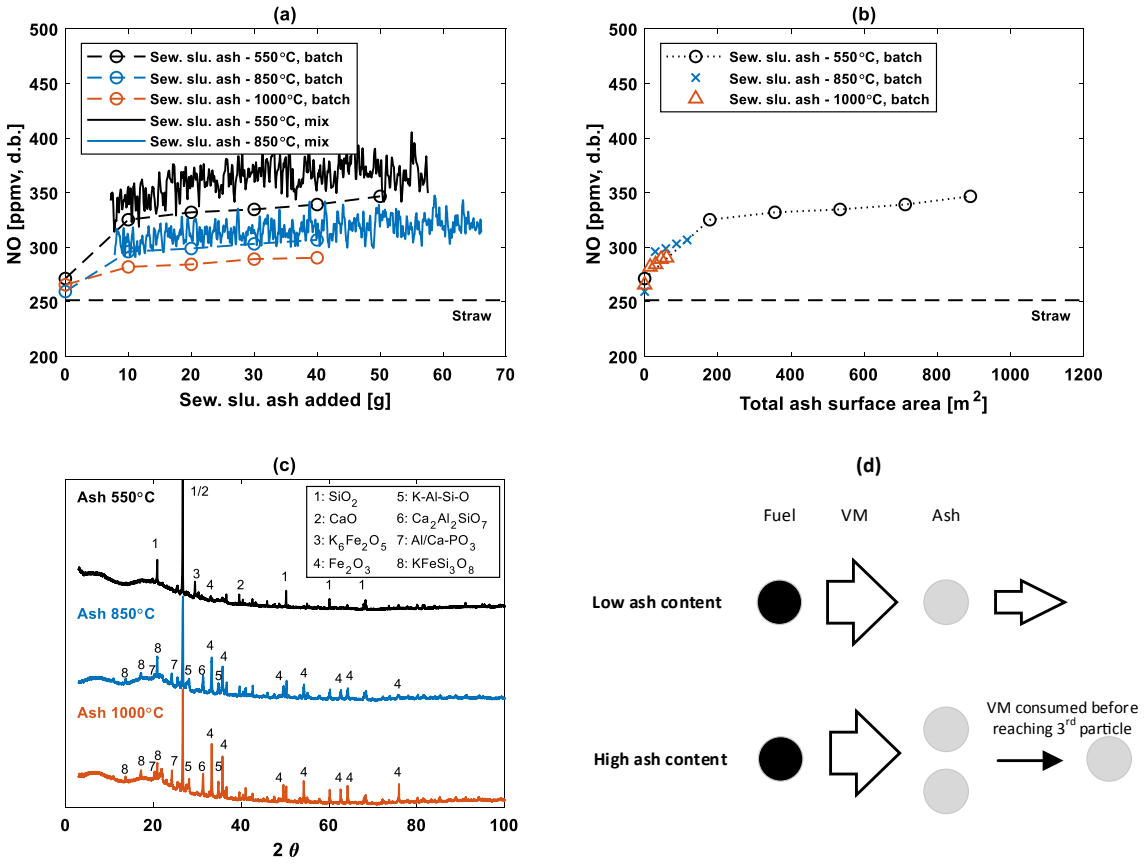

Fig. 4. NO emission (6% O_2) during fluidized bed combustion of straw with sewage sludge ash (batch addition or premixed with fuel) (a), NO emission from batch addition of sewage sludge ash during straw combustion against total available surface area (b), XRD spectra of the employed sewage sludge ash (c), and mechanism of volatile matter (VM) conversion at low and high ash content (d). The straw to sewage sludge ash ratio was 2 kg straw/kg sew. slu. ash in the continuous experiments, and the sew. slu. ash feeding rate was 0.5 g sew. slu. ash/min in all experiments employing ash. Conditions: T_{bed} = 850 °C; λ = 1.4; λ_1/ λ = 1.

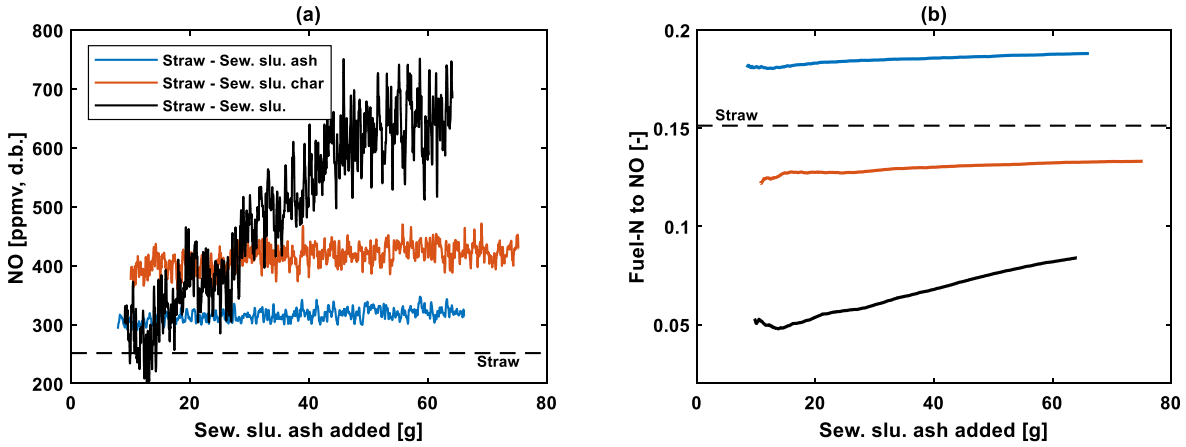

Fig. 5. NO emission (6% O_2) (a) and fuel-N to NO conversion (b) from straw combustion and combustion of straw with sewage sludge fuel, char, or ash. The ash and char were prepared at 850 °C. The straw to sewage sludge ash ratio and ash feeding rate were 2–2.4 kg straw/kg sew. slu. ash and 0.5 g sew. slu. ash/min, respectively. For co-combustion, 50% straw and 50% sewage sludge was used. Conditions: T_{bed} = 850 °C; λ = 1.4; λ_1/ λ = 1.

char reached a steady state after the addition of approximately 10–15 g ash. The combustion of straw with sewage sludge ash increased NO emission and fuel-N to NO conversion, while the straw-sewage sludge char combustion increased NO emission and decreased the fuel-N to NO conversion. The latter increase in NO emission is expected as more nitrogen is introduced the reactor. The decrease in fuel-N to NO conversion may be caused by the lower propensity of sewage sludge char for forming NO or the higher reactivity of sewage sludge char towards NO reduction [18]. In contrast to the steady combustion in the previous cases, the NO emission and fuel-N to NO conversion during co-combustion of the two fuels exhibited a transient behaviour. The NO emission and fuel-N to NO conversion increased with the addition of sewage sludge ash until approximately 50–60 g ash was added, at which the gradient started decreasing. The transient behaviour was conceivably related to the volatiles released from sewage sludge, which affected the preferred oxidation pathway of the introduced nitrogen depending

on the amount of ash present. The mechanisms were further studied by examining the NO reduction reactivity of the fuels along with measurements of the local gas composition.

3.1.2. NO reduction reactivity

The NO reduction in the reactor during combustion was investigated by introducing NO with the primary gas. The fractional reduction of the added NO (R_{NO}) was quantified by Eq. (3) [31]. Here, $C_{NO,in}$ (ppmv) is the inlet concentration of added NO, $C_{NO,c}$ (ppmv) is the NO emission during combustion without addition of NO, and $C_{NO,out}$ (ppmv) is the NO emission with the addition of NO. Raw data of the NO reduction experiments are provided in the supplemental material (Fig. S5).

$$R_{NO} = \frac{C_{NO,in} + C_{NO,c} - C_{NO,out}}{C_{NO,in}} \quad (3)$$

Fig. 6 illustrates R_{NO} against time for straw, and against the amount of added sewage sludge ash for the experiments involving sewage sludge. R_{NO} of straw was stable during steady state combustion until defluidization after about 4200 s. In contrast, R_{NO} decreased for sewage sludge and showed a maximum during co-combustion. The results indicate that the reduction propensity was higher at the early stages of combustion, i.e. lower ash content, and decreased with increasing ash content. After around 40 g of ash introduced to the reactor, the reduction of external NO was similar for the three cases. The relevant NO reduction mechanisms are by char, combustibles (CO and C_XH_Y), and NH_3 or other N-containing light gaseous species. As the char content is approximately constant within the reactor during steady state combustion and the char reactivity is unchanged by ash accumulation as deduced from Fig. 5, the transient behaviour in NO reduction propensity is likely caused by the NO reducing gaseous components such as light gas nitrogen or combustibles. At low concentrations of ash in the reactor, NH_3 (and possibly HCN) may favour the reduction of NO, thereby explaining the higher reduction reactivity. With the accumulation of ash, the light gaseous N-species are oxidized to NO catalysed by sewage sludge ash. The ash could possibly also influence the concentration of combustibles, e.g. by catalysing oxidation reactions of CH_4 and CO [28], the presence of which could affect the NO reduction indirectly (change in thermal $DeNO_X$) or directly (reburning mechanism). The influence of sewage sludge ash on the light gaseous species from combustion was further examined by local gas composition measurements.

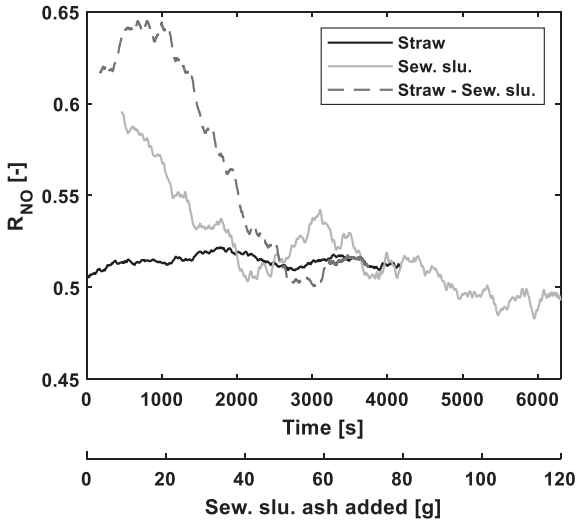

Fig. 6. Fractional NO reduction (R_{NO}) against time for straw, and against sewage sludge ash added for experiments involving sewage sludge. For co-combustion, 50% straw and 50% sewage sludge was used. Conditions: T_{bed} = 850 °C; λ = 1.4; $\lambda_1/\lambda = 1$, NO_{in} = 1600ppmv.

3.1.3. Local gas composition measurements

Fig. 7 depicts the experimental NO and NH_3 axial concentration profiles during co-combustion of straw and sewage sludge. Measurements for the co-combustion were taken at the initial stages of combustion, corresponding to 2 – 25 g of sewage sludge ash added, while the late measurements were taken from 40 to 80 g sewage sludge ash added. The profiles indicate that the combustion reactions predominantly occurred between the top of the dense bed and fuel inlet. In addition, the concentration of gaseous species in the bed was inhomogeneous, suggesting a low fuel turnover. At low levels of ash in the reactor, a larger amount of NH_3 and correspondingly lower concentration of NO were detected at the top of the bed. With the accumulation of ash, the maximum in the NO and NH_3 profiles shifted due to the increase in bed height. The increased ash content additionally lowered the NH_3 and increased the NO concentration at the top of the bed and in the freeboard. Moreover, the accumulation of ash shifted the C_XH_Y and CO concentration profiles without significantly altering their magnitudes, shown in the supplemental material (Figs. S6 and S7). Consequently, the observed behavior in NO may be attributed to the light gas-N chemistry. As HCN was not measured, this is not included in the following discussion. However, it is presumed based on previous studies that the oxidation of HCN would be promoted in the presence of biomass ash and Ca-compounds, similar to that of NH_3 [21,28,32]. While the presence of ash may affect the formation and reduction reactions of NO, the results using model compounds (Fig. 4) suggest that sewage sludge ash promotes the formation of NO from NH_3 (R1) and HNCO (R2), likely due to the large Fe and Ca contents [21,22,32,33]. Some HNCO was observed during the early stages of co-combustion (Fig. S8), which was not detectable at later stages. This along with the decrease in NH_3 concentration with ash accumulation suggest that the transient behavior of the NO concentration is related to the catalytic formation of NO. The reduced concentration of NH_3 at high ash content further reduced the propensity of thermal $DeNO_X$ reactions in the freeboard, ultimately leading to an increased NO emission.

$$NH_3 + 5/4\ O_2 \xrightarrow{\text{Sew.slu.ash}} NO + 3/2\ H_2O \quad (R1)$$

$$HNCO + 5/4\ O_2 \xrightarrow{\text{Sew.slu.ash}} NO + CO + 1/2\ H_2O \quad (R2)$$

The freeboard chemistry was further examined using the nitrogen model of Glarborg et al. [34]. Assuming no elutriation of char and ash particles, the freeboard chemistry was modelled as a plug flow reactor. The initial conditions of the simulations are summarized in Table S1. The modelled and experimental data are compared in Fig. 8, showing that the NH_3 concentration was well predicted, while a significant difference was observed between the modelled and experimental NO concentration. Besides differences in magnitude, the model predicted a fast completion of the ongoing reactions, while the experimental data exhibited a gradual change. There may be several causes for these deviations, the most important of which are the invasive nature of the probe experiments, the influence of radiation on temperature measurements, the oversimplification of flow pattern, and the influence of trace species, and elutriated char and ash. The first two factors are related to temperature variation, which affects the nitrogen chemistry considerably. The actual gas temperature in the reactor may be lower due to the influence of radiation from the external heating on the thermocouple. Moreover, the cooling of the probe may have affected the gas temperature below the measurement point. The influence of temperature on the modelling results is demonstrated in the supplemental material (Fig. S9), showing that NO reduction was facilitated at a lower temperature. For the flow pattern, more complicated fluid dynamic models are necessary, as the assumption of plug flow may not be

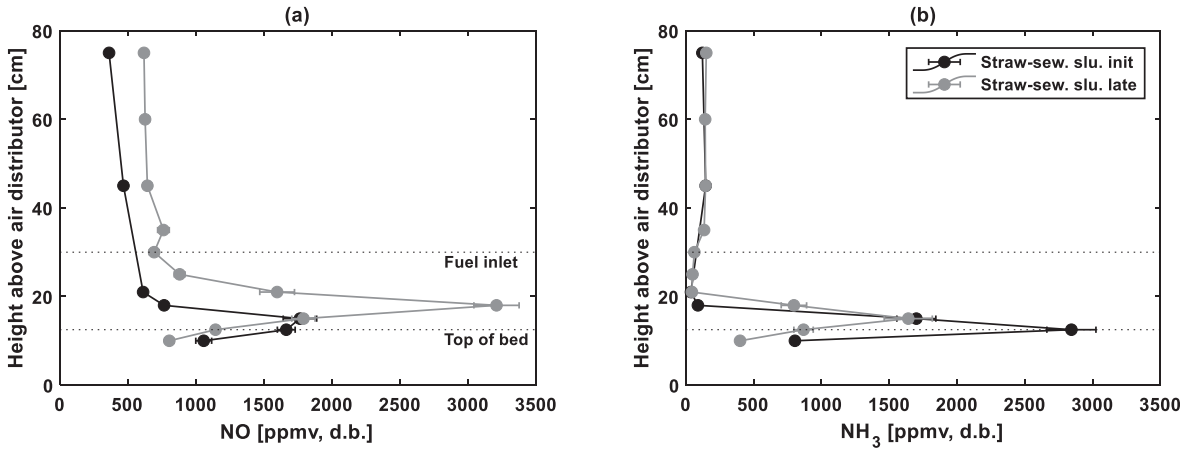

Fig. 7. Experimental axial NO (a) and NH_3 (b) profiles during fluidized bed co-combustion of 50% straw and 50% sewage sludge. The error bars indicate temporal fluctuations in the concentration. Initial stage (init) corresponds to the addition of 2–25 g of ash, while late stage (late) corresponds to the addition of 40–80 g of ash to the reactor. Conditions: T_{bed} = 850 °C; λ = 1.4; λ_1/λ = 1.

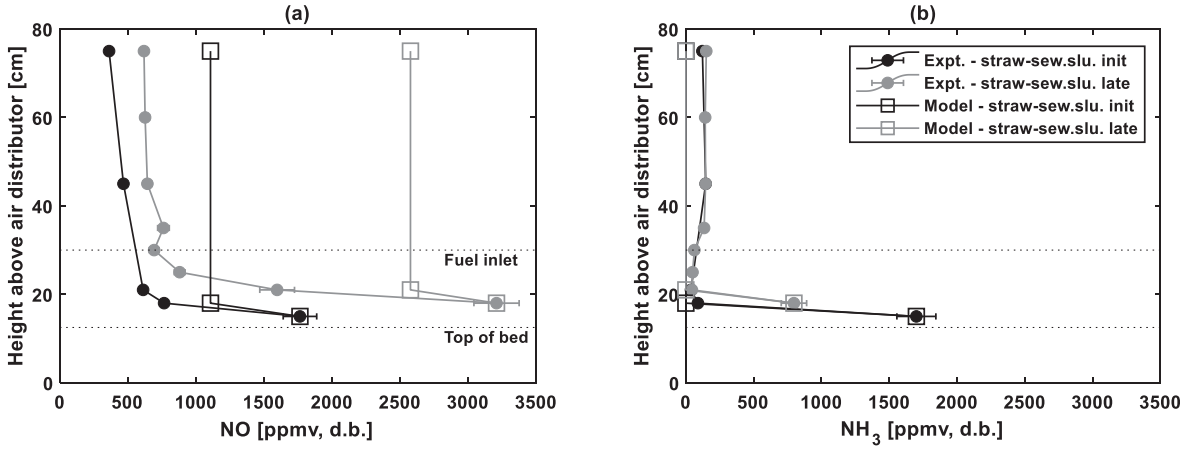

Fig. 8. Experimental and modelled NO (a) and NH_3 (b) axial concentration profiles in the freeboard during fluidized bed co-combustion of 50% straw and 50% sewage sludge. Initial stage (init) corresponds to the addition of 2–25 g of ash, while late stage (late) corresponds to the addition of 40–80 g of ash to the reactor. Simulations were performed in Chemkin using the model of Glarborg et al. [34], described in the supplemental material. Experimental conditions: T_{bed} = 850 °C; λ = 1.4; λ_1/λ = 1.

applicable in the fluid bed reactor due to bubble bursting, and mixing of primary and secondary gas streams. Lastly, the presence of trace species such as K/Na, S, and Cl compounds [30], and of elutriated char and ash may additionally affect the nitrogen chemistry in the freeboard, which was not accounted for in the model. While the experiments were performed at a relatively low primary gas velocity (u/u_{mf} = 4), elutriated char and ash particles should be taken into account below the Transport Disengaging Height (TDH). Nonetheless, the simulation results qualitatively predict the reduction of NO in the freeboard. The NO reduction in the initial stages (38%) of combustion is more significant than later (19%), due to the higher concentration of NH_3.

3.2. Air staged combustion

Fig. 9 illustrates the averaged NO emission during combustion of straw, sewage sludge, and their mixtures at air staged and unstaged conditions. The average NO emission ($C_{NO,average}$) for a given mixing ratio and air staging configuration demonstrates the changes with time as calculated from Eq. (4). In eq. (4), $C_{NO,average}$ is calculated as a moving/cummulative average from 0 s to (1200 i) s. As the combustion time differed between around 1–2 h for the experiments, different values of the index *i* was used. The last point for a given mixing ratio and air staging configuration corresponds to the overall average, and is

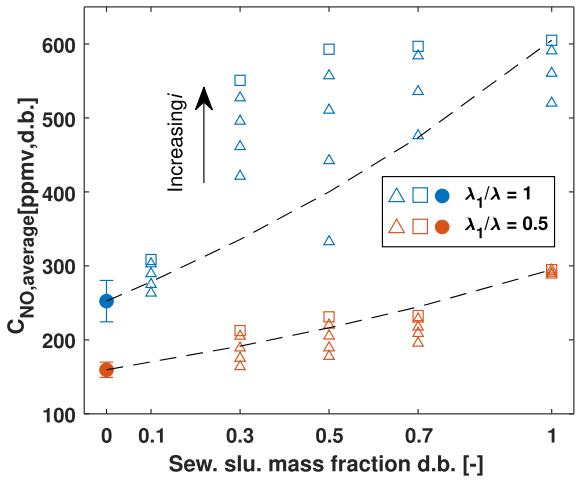

Fig. 9. Averaged NO emission (6% O_2) during fluidized bed co-combustion of straw and sewage sludge at air staged and unstaged conditions. The overall average is shown with a square. Conditions: T_{bed} = 850 °C, λ = 1.4, λ_1/λ = 0.5 and 1.

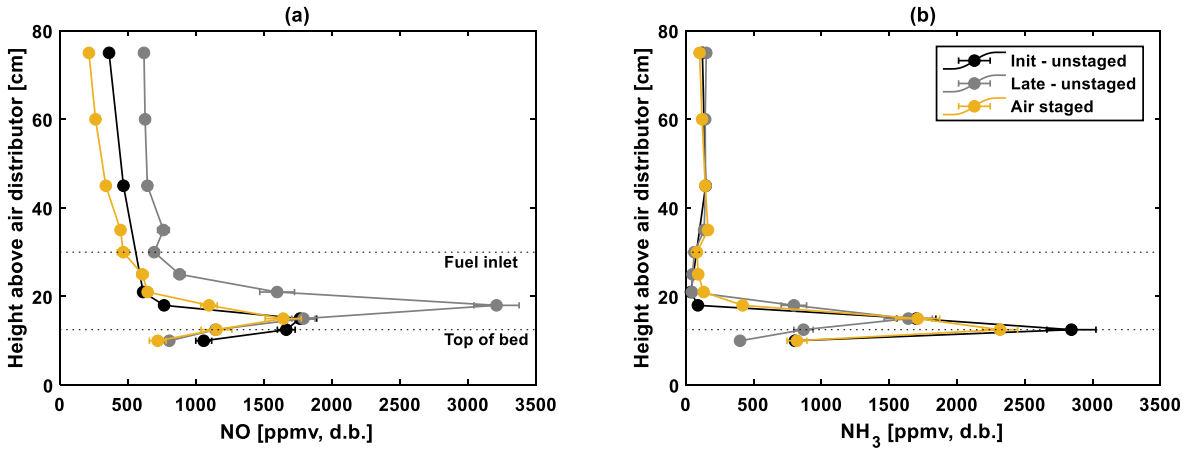

Fig. 10. Experimental axial NO (a) and NH_3 (b) profiles during fluidized bed co-combustion of 50% straw and 50% sewage sludge under air staged and unstaged conditions. Initial stage (init) corresponds to the addition of 2–25 g of ash, while late stage (late) corresponds to the addition of 40–80 g of ash to the reactor. Conditions: T_{bed} = 850 °C; λ = 1.4; λ_1/λ = 0.5 and 1.

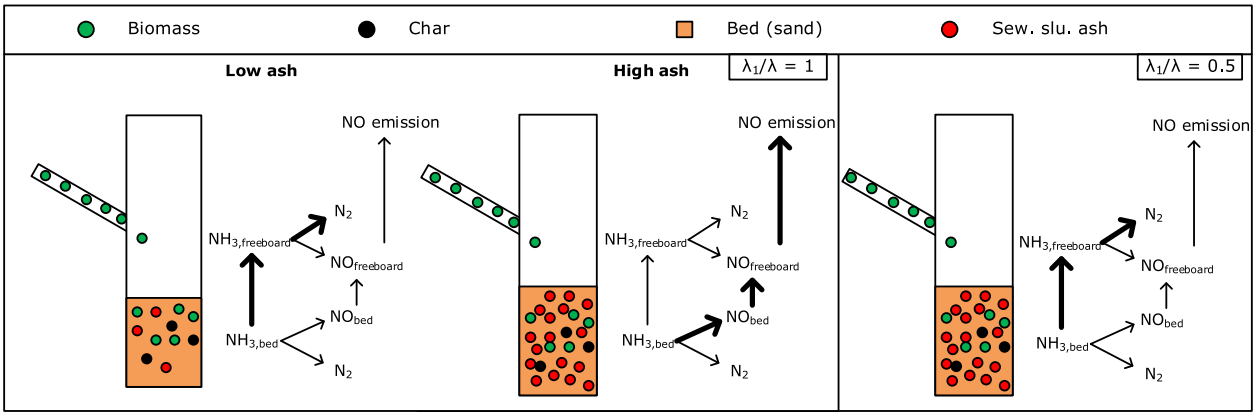

Fig. 11. Illustration of the influence of sewage sludge ash on the nitrogen chemistry during air staged and unstaged co-combustion of straw and sewage sludge. The thicker arrows shows the preferred reaction pathways. λ_1/λ is the fraction of total air introduced as primary air, i.e. from the bottom.

illustrated with a square. Additionally, an evenly spaced averaging was employed in the supplemental material (Fig. S10), from which similar inferences can be drawn. The results in Fig. 9 show that at air unstaged conditions, the NO concentration changed significantly with time (increasing *i*). This change was less prominent in the later stages of combustion, likely due to a saturation mechanism similar to that shown in Fig. 4d. In comparison, the change in NO was much less pronounced at air staged conditions, most likely due to the lower concentration of O_2 and thereby lower importance of NO forming catalytic reactions near the bed and freeboard. Instead, the high Fe content of sewage sludge ash could promote NH_3 decomposition to N_2 under reducing conditions [35]. However, the form and reactivity of the ash under reducing conditions may be different, which would require further study. For all cases, air staging led to a significant reduction in NO emission (40–60%).

$$C_{NO,average}(0\text{ s to }1200\cdot i\text{s}) = \int_{t=0}^{t=i\cdot 1200\text{ s}} C_{NO}(t)\ \ dt \quad \text{with} \quad i = 1, 2, 3, \ldots \qquad (4)$$

3.2.1. Local gas composition measurements

The NO and NH_3 axial concentration profiles during straw-sewage sludge co-combustion are depicted in Fig. 10 at air staged and unstaged conditions. The NO and NH_3 profiles during air staged combustion were similar to those obtained during the initial stages of unstaged combustion, i.e. relatively low NO and high NH_3 were detected near the bed. However, in contrast to the unstaged experiment, negligible changes to the concentration profiles were observed during staged combustion up to the addition of approximately 60 g of sewage sludge ash. This further indicates that the catalytic formation of NO was of lesser importance when the bottom section of the fluidized bed reactor was kept under reducing conditions. The low O_2 concentration also resulted in a generally higher CO concentration below the fuel inlet, demonstrated in the supplemental material (Fig. S11). This ultimately led to an increased CO emission from the reactor, an often natural consequence of employing staged combustion.

3.3. Mechanism of interaction in combustion with sewage sludge (high-ash fuels)

During straw-sewage sludge co-combustion, a synergy effect was observed (Fig. 2). This was attributed to the catalytic effect of sewage sludge ash, which could catalyse the formation of NO from NH_3 and HNCO (Fig. 3), and possibly HCN [21]. The catalytic effect of the ash depended on the ash preparation temperature and the mixing with the fuel (Fig. 4). During straw-sewage sludge co-combustion, the NO emission increased with the accumulation of sewage sludge ash. This transient trend was not observed in combustion of straw with sewage sludge ash and char (Fig. 5). The transient NO emission was primarily attributed to the influence of sewage sludge ash on the volatile N-chemistry, as ash accumulation had little effect on the CO and C_XH_y profiles during co-combustion. The influence of sewage sludge ash on the nitrogen chemistry is simplistically illustrated in Fig. 11, showing the pathways of

NH_3 oxidation. Notably, HNCO would and HCN may react in a similar manner. Under air unstaged conditions, when the ash content in the bed is low, the catalytic oxidation of NH_3 to NO was of lesser importance, and a larger amount of NH_3 was observed in the bed, which increased the potential for NO reduction by thermal $DeNO_X$. At a high ash content, a significantly higher amount of NO was formed in the bed due to the catalytic oxidation of NH_3. In conjunction with the lower concentration of NH_3 in the freeboard, this ultimately led to a high NO emission. At air staged conditions, the NO emission did not change significantly with ash accumulation, attributed to the lower O_2 concentration and thereby lower importance of NO forming catalytic reactions near the bed and freeboard. Hence, air staging could be an efficient technique to minimize the catalytic oxidation of volatile nitrogen to NO during combustion with sewage sludge.

To provide further insight into the influence of sewage sludge ash on the gaseous chemistry, fundamental studies are necessary. It was noted that the catalytic activity of the ash decreased with increasing ash preparation temperature (Fig. 4). This was caused by the decrease in surface area with increasing ash preparation temperature. In addition, differences in the ash composition (crystal structure) may additionally influence the ash reactivity, which would require further fundamental study. Moreover, the reduction potential decreased with increasing ash accumulation (Fig. 6), which was attributed to a change in the preferred oxidation pathway of NH_3. Insight into the influence of ash and other trace species on a fundamental level would require further study. In addition, the catalytic effect of the ash was characterized at a single temperature and further work at different temperatures would be desirable. Temperature affects the preferred reaction pathways of NH_3 and an optimum, commonly observed in selective catalytic reduction (SCR) [36], may occur.

4. Conclusions

The influence of biomass co-combustion on NO_X emissions was investigated in a lab-scale fluidized bed reactor. The NO emission from straw-sunflower seed and straw-sunflower husk co-combustion was additive based on effluent NO measurements, while a synergy effect was observed during straw-sewage sludge co-combustion. This was primarily caused by the promotional effect of sewage sludge ash on NO formation from NH_3 and HNCO, and possibly HCN. The catalytic reactivity of the ash towards NO formation increased with a lower ash preparation temperature and a better mixing of ash with straw. The influence of temperature was attributed to the higher surface area of the low temperature ash and possibly to differences in the crystal composition as determined by XRD.

In the initial stages of straw-sewage sludge co-combustion, the NH_3 released by sewage sludge reduced the NO emission, while at higher concentration of ash in the bed, the NH_3 was predominantly oxidized to NO. Consequently, the observed interaction in the nitrogen chemistry of straw and sewage sludge involved both homogeneous and heterogeneous pathways.

Air-staging significantly reduced the NO emissions from combustion. In addition, the interaction effect between straw-sewage sludge was less pronounced at air staged conditions. This may be caused by the lower concentration of O_2 near the bed and thereby lower importance of NO forming reactions.

CRediT authorship contribution statement

Burak Ulusoy: Conceptualization, Methodology, Investigation, Visualization. **Bozidar Anicic:** Conceptualization, Methodology, Investigation. **Weigang Lin:** Conceptualization, Methodology, Funding acquisition, Project administration. **Bona Lu:** Conceptualization, Supervision, Project administration. **Wei Wang:** Conceptualization, Supervision, Project administration. **Kim Dam-Johansen:** Conceptualization, Methodology, Funding acquisition, Project administration. **Hao Wu:** Conceptualization, Methodology, Funding acquisition, Project administration.

Declaration of Competing Interest

The authors declare that they have no known competing financial interests or personal relationships that could have appeared to influence the work reported in this paper.

Acknowledgements

This project is funded by the Sino-Danish Centre for Education and Research and Technical University of Denmark.

Appendix A. Supplementary data

Supplementary data to this article can be found online at https://doi.org/10.1016/j.fuel.2021.120431.

References

[1] Sander B. Properties of Danish Biofuels and the Requirements for Power Production. Biomass Bioenergy 1997;12:177–83.
[2] Chen W, Yang H, Chen Y, Li K, Xia M, Chen H. Influence of Biochar Addition on Nitrogen Transformation during Copyrolysis of Algae and Lignocellulosic Biomass. Environ Sci Technol 2018;52:9414–521. https://doi.org/10.1021/acs.est.8b02485.
[3] Ravishankara AR, Daniel JS, Portmann RW. Nitrous Oxide (N2O): The Dominant Ozone-Depleting Substance Emitted in the 21st Century. Science (80-) 2009;326:123–5. 10.1126/science.1176985.
[4] Wang Y, Zhou Y, Bai N, Han J. Experimental investigation of the characteristics of NOx emissions with multiple deep air-staged combustion of lean coal. Fuel 2020;280:118416. https://doi.org/10.1016/j.fuel.2020.118416.
[5] Khan AA, de Jong W, Jansens PJ, Spliethoff H. Biomass combustion in fluidized bed boilers: Potential problems and remedies. Fuel Process Technol 2009;90:21–50. https://doi.org/10.1016/j.fuproc.2008.07.012.
[6] Hupa M, Karlström O, Vainio E. Biomass combustion technology development - It is all about chemical details. Proc Combust Inst 2017;36:113–34. https://doi.org/10.1016/j.proci.2016.06.152.
[7] Sahu SG, Chakraborty N, Sarkar P. Coal-biomass co-combustion: An overview. Renew Sustain Energy Rev 2014;39:575–86. https://doi.org/10.1016/j.rser.2014.07.106.
[8] Kumar R, Singh RI. An investigation of co-combustion municipal sewage sludge with biomass in a 20 kW BFB combustor under air-fired and oxygen-enriched condition. Waste Manag 2017;70:114–26. https://doi.org/10.1016/j.wasman.2017.09.005.
[9] Wu H, Pedersen AJ, Glarborg P, Frandsen FJ, Dam-Johansen K, Sander B. Formation of fine particles in co-combustion of coal and solid recovered fuel in a pulverized coal-fired power station. Proc Combust Inst 2011;33:2845–52. https://doi.org/10.1016/j.proci.2010.06.125.
[10] Wu H, Glarborg P, Frandsen FJ, Dam-Johansen K, Jensen PA, Sander B. Co-combustion of pulverized coal and solid recovered fuel in an entrained flow reactor - General combustion and ash behaviour. Fuel 2011;90:1980–91. https://doi.org/10.1016/j.fuel.2011.01.037.
[11] Lu L, Jin Y, Liu H, Ma X, Yoshikawa K. Nitrogen evolution during the co-combustion of hydrothermally treated municipal solid waste and coal in a bubbling fluidized bed. Waste Manag 2014;34:79–85. https://doi.org/10.1016/j.wasman.2013.08.025.
[12] Abelha P, Gulyurtlu I, Cabrita I. Release of nitrogen precursors from coal and biomass residues in a bubbling fluidized bed. Energy Fuels 2008;22:363–71. https://doi.org/10.1021/ef700430t.
[13] Fryda L, Panopoulos K, Vourliotis P, Kakaras E, Pavlidou E. Meat and bone meal as secondary fuel in fluidized bed combustion. Proc Combust Inst 2007;31:2829–37. https://doi.org/10.1016/j.proci.2006.07.151.
[14] Liu DC, Mi T, Shen BX, Feng B, Franz W. Reducing N2O emission by Co-combustion of coal and biomass. Energy Fuels 2002;16:525–6. https://doi.org/10.1021/ef010108f.
[15] Leckner B, Karlsson M. Gaseous emissions from circulating fluidized bed combustion of wood. Biomass Bioenergy 1993;4:379–89.
[16] Robinson AL, Junker H, Buckley SG, Sclippa G, Baxter LL. Interactions between coal and biomass when cofiring. Proc Combust Inst 1998;27:1351–9. https://doi.org/10.1016/S0082-0784(98)80540-7.
[17] Areeprasert C, Scala F, Coppola A, Urciuolo M, Chirone R, Chanyavanich P, et al. Fluidized bed co-combustion of hydrothermally treated paper sludge with two coals of different rank. Fuel Process Technol 2016;144:230–8. https://doi.org/10.1016/j.fuproc.2015.12.033.
[18] Ulusoy B, Wu H, Lin W, Karlström O, Li S, Song W, et al. Reactivity of sewage sludge, RDF, and straw chars towards NO. Fuel 2019;236:297–305. https://doi.org/10.1016/j.fuel.2018.08.164.

[19] Ulusoy B, Lin W, Karlström O, Li S, Song W, Glarborg P, et al. Formation of NO and N_2O during raw and demineralized biomass char combustion. Energy Fuels 2019. https://doi.org/10.1021/acs.energyfuels.9b00622.
[20] Shimizu T, Toyono M, Ohsawa H. Emissions of NO_X and N_2O during co-combustion of dried sewage sludge with coal in a bubbling fluidized bed combustor. Fuel 2007; 86:957–64. https://doi.org/10.1016/j.fuel.2006.10.001.
[21] Shimizu T, Toyono M. Emissions of NOx and N2O during co-combustion of dried sewage sludge with coal in a circulating fluidized bed combustor. Fuel 2007;86: 2308–15. https://doi.org/10.1016/j.fuel.2007.01.033.
[22] Cammarota A, Chirone R, Salatino P, Solimene R, Urciuolo M. Particulate and gaseous emissions during fluidized bed combustion of semi-dried sewage sludge: Effect of bed ash accumulation on NOx formation. Waste Manag 2013;33: 1397–402. https://doi.org/10.1016/j.wasman.2013.02.016.
[23] Hartman M, Svoboda K, Pohořelý M, Trnka O. Combustion of dried sewage sludge in a fluidized-bed reactor. Ind Eng Chem Res 2005;44:3432–41. https://doi.org/10.1021/ie040248n.
[24] Koebel M, Strutz EO. Thermal and hydrolytic decomposition of urea for automotive selective catalytic reduction systems: Thermochemical and practical aspects. Ind Eng Chem Res 2003;42:2093–100. https://doi.org/10.1021/ie020950o.
[25] Sato N, Quitain AT, Kang K, Daimon H, Fujie K. Reaction Kinetics of Amino Acid Decomposition in High-Temperature and High-Pressure Water. Ind Eng Chem Res 2004;43:3217–22. https://doi.org/10.1021/ie020733n.
[26] Lin W, Johnsson JE, Dam-Johansen K, van den Bleek CM. Interaction between emissions of sulfur dioxide and nitrogen oxides in fluidized bed combustion. Fuel 1994;73:1202–8.
[27] Köpsel RFW, Halang S. Catalytic influence of ash elements on NOx formation in char combustion under fluidized bed conditions. Fuel 1997;76:345–51. https://doi.org/10.1016/S0016-2361(96)00231-1.
[28] Löffler G, Wargadalam VJ, Winter F. Catalytic effect of biomass ash on CO, CH4 and HCN oxidation under fluidised bed combustor conditions. Fuel 2002;81:711–7. https://doi.org/10.1016/S0016-2361(01)00203-4.
[29] Wang G, Jensen PA, Wu H, Frandsen FJ, Laxminarayan Y, Sander B, et al. Potassium capture by coal fly ash: K2CO3, KCl and K2SO4. Fuel Process Technol 2019;194:106–15. https://doi.org/10.1016/j.fuproc.2019.05.038.
[30] Glarborg P. Hidden interactions-Trace species governing combustion and emissions. Proc Combust Inst 2007;31 I:77–98.. https://doi.org/10.1016/j.proci.2006.08.119.
[31] de Diego LF, de las Obras-Loscertales M, Rufas A, García-Labiano F, Gayán P, Abad A, et al. Pollutant emissions in a bubbling fluidized bed combustor working in oxy-fuel operating conditions: Effect of flue gas recirculation. Appl Energy 2013;102: 860–7. https://doi.org/10.1016/j.apenergy.2012.08.053.
[32] Shimizu T, Satoh M, Fujikawa T, Tonsho M. Simultaneous Reduction of SO2, NOX, and N2O Emissions from a Two-Stage Bubbling Fluidized Bed Combustor. Energy Fuels 2000;14:862–8. https://doi.org/10.1021/ef9902202.
[33] Åmand L-E, Leckner B, Dam-Johansen K. Influence of SO_2 on the NO/N_2O chemistry in fluidized bed combustion. Fuel 1993;72:557–64. https://doi.org/10.1016/0016-2361(93)90116-J.
[34] Glarborg P, Miller JA, Ruscic B, Klippenstein SJ. Modeling nitrogen chemistry in combustion. Prog Energy Combust Sci 2018;67:31–68. https://doi.org/10.1016/j.pecs.2018.01.002.
[35] Fu SL, Song Q, Yao Q. Experimental and kinetic study on the influence of iron oxide on the selective noncatalytic reduction DeNOx process. Ind Eng Chem Res 2014;53: 5801–9. https://doi.org/10.1021/ie500109r.
[36] Chmielarz L, Jabłońska M. Advances in selective catalytic oxidation of ammonia to dinitrogen: A review. RSC Adv 2015;5:43408–31. https://doi.org/10.1039/c5ra03218k.